AUTOMATIC SEGMENTATION OF BRAIN STRUCTURES FROM MRI INTEGRATING ATLAS-BASED LABELING AND LEVEL SET METHOD

Matineh Shaker[1], *Hamid Soltanian-Zadeh*[1-2]

[1] Control and Intelligent Processing Center of Excellence, Department of Electrical and Computer Engineering, University of Tehran, Tehran, Iran
m.shaker@ece.ut.ac.ir, hszadeh@ut.ac.ir

[2] Image Analysis Lab., Department of Radiology, Henry Ford Hospital, Detroit, Michigan, USA
hamids@rad.hfh.edu

ABSTRACT

The purpose of this study is to segment hippocampus, amygdala and entorhinal cortex in magnetic resonance images (MRI) of temporal lobe epilepsy (TLE) patients. The proposed method consists of two separate parts. First, we use an atlas-based segmentation method to obtain initial segmentation results for desired structures. Using additional preprocessing steps for image registration and gray matter (GM) segmentation is the specification of this stage of the work. Then, all of the GM voxels are labeled using an anatomical atlas. In the next stage, variational level set formulation without re-initialization is applied on the images. We use the boundaries obtained by atlas-based segmentation as the contour for initialization of level set function. Automatic generation of initial contour makes the final segmentation results operator-independent. The proposed approaches are evaluated by comparing automatic and expert's segmentation results and confirming their similarity.

Index Terms— Image segmentation, level set method, atlas-based segmentation, magnetic resonance images, curve initialization

1. INTRODUCTION
2.

The structures that appear in magnetic resonance images (MRI) are often segmented for a variety of clinical and research applications. Many neurodegenerative diseases show changes in volume and shape of brain structures. In this application, segmentation of specific brain structures has clinical values in diagnosis stage, decision about surgeries and treatment evaluations [1],[2]. Manual delineation of brain structures suffer from difficulties of defining anatomical landmarks and boundaries, as well as obtaining results with low reproducibility and objectivity.

In this study, we focus on automatic segmentation of brain structures from MR images of temporal lobe epilepsy (TLE) patients. Among all of the brain structures, those in the temporal lobe of the brain are most affected by TLE. We develop automatic methods for the segmentation of the hippocampus, amygdala, and entorhinal cortex which are among the most challenging structures in the brain to segment.

First, preprocessing stages are applied to the image data. These steps include spatial normalization, gray matter (GM) segmentation, exclusion of non-brain voxels, and compensation of spatial normalization effects. Then, all of the gray matter voxels are labeled using an anatomical atlas to create individual regions for each of the brain structures. By making the maximum probability atlas, corresponding voxels of the desired structures are obtained. In the next stage, we use the level set framework proposed in [3] to obtain more precise segmentation results.

Novel contributions of this work are two-fold. First, we use a specific atlas-based segmentation procedure for generating the initial contour for the level set method. Secondly, we segment the entorhinal cortex automatically. To our knowledge, none of the previous studies segmented this structure automatically.

The rest of the paper is organized as follows. In Section 2, the specification of data and image acquisition protocol are described. Also, our proposed method for generating the initial contour and segmentation of the structures are presented. Section 3 presents the segmentation results and evidences for their accuracy. Finally, Section 4 concludes the paper.

2. MATERIALS AND METHODS

2.1. Image Acquisition and Subjects

Magnetic resonance images were acquired using a General Electric 3 Tesla Signa system (GE Medical System,

Milwaukee, WI). All patients underwent coronal T1-weighted MRI study using a spoiled gradient-echo (SPGR) sequence with $TR/TI/TE = 7.6/1.7/500ms$, flip angle = 20°, field of view (FOV) = $200 \times 200mm^2$, matrix size = 256×256, pixel size = $0.781 \times 0.781mm^2$, and slice thickness = $2.0mm$. Six subjects were included in this study (4 female, 2 male). They are adults with an age average and standard deviation of 41 and 11 years, respectively.

2.2. Preprocessing

In this section, we describe the preprocessing stages applied before the actual segmentation of the brain structures. These are performed using SPM5 (Wellcome Department of Imaging Neuroscience, London, UK; www.fil.ion.ucl.ac.uk).

1) Intensity non-uniformity correction. The images are corrected for the bias effects. The MR images are usually affected by smooth artifacts that are not problems for visual inspection, but can make problems for automated procedures.

2) Spatial normalization. Image registration to an atlas is a common framework with the introduction of statistical methods for image processing, such as statistical parametric mapping (SPM) [4]. We use a well-known probabilistic atlas from the Montreal Neurological Institute (MNI). We register all of the structural images to the MNI template using 12 parameter affine transformation and obtain transformation matrix which is needed for atlas-based segmentation.

3) Gray mater segmentation. Since hippocampus, amygdale, and entorhinal cortex are all gray matter (GM) structures, normalized images are segmented to gray matter partitions. This segmentation is performed by the probability maps, used as Bayesian priors.

4) Exclusion of nonbrain voxels. According to the method proposed in [5], all of the GM images are eroded to remove nonbrain voxels from the skull, scalp, and venous sinuses. The erosion is followed by conditional dilation. The obtained images are extracted gray matter partitions in the stereotactic space.

5) Modulation. Spatial normalization may cause some specific regions of the brain to grow and other regions to shrink. For instance, if a subject's structures have very different from the template, then the volumes change dramatically during the normalization step. This effect can be compensated by multiplying voxel values of spatially normalized gray matter images by relative volume of gray matter before and after normalization. The changes of regions in the normalized image in relation to the original image make a deformation field. The gradient of this deformation field is its Jaccobian matrix and consists of the following matrix in the 3D space:

$$\begin{bmatrix} \frac{dx}{dx'} & \frac{dx}{dy'} & \frac{dx}{dz'} \\ \frac{dy}{dx'} & \frac{dy}{dy'} & \frac{dy}{dz'} \\ \frac{dz}{dx'} & \frac{dz}{dy'} & \frac{dz}{dz'} \end{bmatrix} \quad (1)$$

where $[x\ y\ z]$ and $[x'\ y'\ z']$ are the coordinate vectors in the original and normalized images, respectively. We can use the determinant of the Jaccobian matrix as a measure of relative volumes of the GM before and after normalization.

2.3. Atlas-Based Segmentation

To obtain a rough segmentation of brain structures, each individual gray mater voxel is labeled based on the MNI atlas and the transformation matrix gained in preprocessing step. Then, by computing the voxel by voxel average of the same structure label from a group of subjects, statistical probability anatomy maps are created. Finally, the label of the most probable structure is stored at each voxel of the maximum probability atlas. We extract the corresponding voxels of the hippocampus, amygdala, and entorhinal cortex and obtain an initial three dimensional segmentation of these structures. In next section, the method that we use to obtain precise segmentation results is described.

2.4. Level Set Segmentation

Level set methods can be formulated as the zero level set $\{(x,y)|\phi(x,y,t)=0\}$ of a time dependent function $\phi(x,y,t)$ that evolves according to the following equation [6]:

$$\frac{\partial \phi}{\partial t} + F|\nabla \phi| = 0 \quad (2)$$

where F is the speed function, which depends on the image data and the level set function ϕ. In the traditional level set methods [7], the level set function can develop steep or flat shapes during its evolution, which makes further computation inaccurate. To avoid this problem, the function ϕ is initialized as a signed distance function. Then, it is re-initialized during the evolution by solving the following equation [8]:

$$\frac{\partial \phi}{\partial t} = sign(\phi_0)(1 - |\nabla \phi|) \quad (3)$$

where ϕ_0 is the function that is re-initialized and $sign(\phi)$ is the sign function. If ϕ_0 is not smooth, the zero level set of the function ϕ is moved incorrectly away from that of the original function [3],[9]. Note that in these methods, the level set function should not be far from a signed distance function.

To avoid these problems, we use a variational level set formulation without re-initialization proposed in [3]. Also, we use our atlas-based segmentation results as the contour for initialization of function ϕ before the evolution. For image I, the edge indicator function is defined by:

$$g = \frac{1}{1+\left|\nabla G_\sigma * I\right|^2} \tag{4}$$

where G_σ is the Gaussian kernel with standard deviation σ. The external energy that moves the zero level set function towards the desired image features like boundaries is defined as:

$$\varepsilon_{g,\lambda,\nu}(\phi) = \lambda\varphi_g(\phi) + \nu\gamma_g(\phi) \tag{5}$$

where λ and ν are constants, and $\varphi_g(\phi)$ and $\gamma_g(\phi)$ are defined by following equations:

$$\varphi_g(\phi) = \int_\Omega g\delta(\phi)\left|\nabla\phi\right|dxdy \tag{6}$$

$$\gamma_g(\phi) = \int_\Omega gH(-\phi)dxdy \tag{7}$$

where δ is the Dirac function, H is the Heaviside function, and $\Omega \in \Re^2$ is the image space. The internal energy is another term in the energy function of dynamic curves that prevents function ϕ to be far away from a signed distance function. The proposed method in [3] considers the following internal energy.

$$\rho(\phi) = \int_\Omega \frac{1}{2}(\left|\nabla\phi - 1\right|)^2 dxdy \tag{8}$$

Finally, the total energy function is defined as:

$$\varepsilon(\phi) = \mu\rho(\phi) + \varepsilon_{g,\lambda,\nu}(\phi) \tag{9}$$

By minimizing the above equation, the zero level set function ϕ is evolved to converge to the object boundaries.

3. RESULTS

We have applied the proposed method to the coronal MR images to segment the hippocampus, amygdala, and entorhinal cortex. Figures 1-3 show the segmentation results. The atlas-based segmentation results, final level set segmentation results, and manually segmented images are shown. We use manually segmented images by an expert to evaluate the automatic segmentation results.

To obtain a quantitative measure, we have calculated the Dice's coefficient as a similarity measure:

$$s = \frac{2\left|X \cap Y\right|}{\left|X\right| + \left|Y\right|} \tag{10}$$

where X and Y are the sets that we want to measure their similarity. For measuring the similarity between automatic segmentation and expert's segmentation, we used the following measure:

$$s = \frac{2n_{overlap}}{n_{automatic} + n_{manual}} \tag{11}$$

where $n_{automatic}$ is the number of pixels in the structure segmented automatically, n_{manual} is the number of pixels in the structure segmented manually, and $n_{overlap}$ is the number of pixels that belong to both of them. We have measured this coefficient for each of the three structures. For evaluation of the results, the brain slices that include these structures have been selected from MRI studies of each of the six subjects. Table 1 presents the mean and standard deviation of the similarity measures between the automatic and expert's segmentations for the six subjects. Also, we have calculated the similarity measures between the manual segmentation and the segmentation results obtained by the method of [3]. These results are also shown in Table 1 and reflect the superiority of our proposed method.

Table 1. Mean and standard deviation of similarity measures for the left and right hippocampus, amygdala, and entorhinal cortex, as segmented by the automatic method and the expert for brain slices that include these structures, acquired from 6 subjects.

	Average $\pm$ *std* **Atlas-Based Initialization**	*Average* $\pm$ *std* **Manual Initialization**
Right Hippocampus	0.91 ± 0.04	0.87 ± 0.05
Left Hippocampus	0.92 ± 0.03	0.89 ± 0.04
Right Amygdala	0.87 ± 0.06	0.84 ± 0.05
Left Amygdala	0.89 ± 0.06	0.88 ± 0.06
Right entorhinal cortex	0.82 ± 0.05	0.75 ± 0.04
Left entorhinal cortex	0.80 ± 0.06	0.73 ± 0.07
Overall	$\mathbf{0.87 \pm 0.05}$	$\mathbf{0.83 \pm 0.05}$

4. CONCLUSION

In this work, we have integrated the atlas-based segmentation method and the level set framework to obtain accurate segmentation of the three temporal lobe structures critical to TLE. Accurate segmentation is the first and most important step in quantitative evaluation of the brain structures. When segmenting an anatomical structure, having priori information about the shape of the structure and its boundaries can significantly improve the final segmentation results. Priori information about the structures was obtained by registering the images to an atlas and labeling the voxels accordingly. The proposed method has successfully segmented the entorhinal cortex which is a very small and difficult-to-segment structure in the coronal view of the brain.

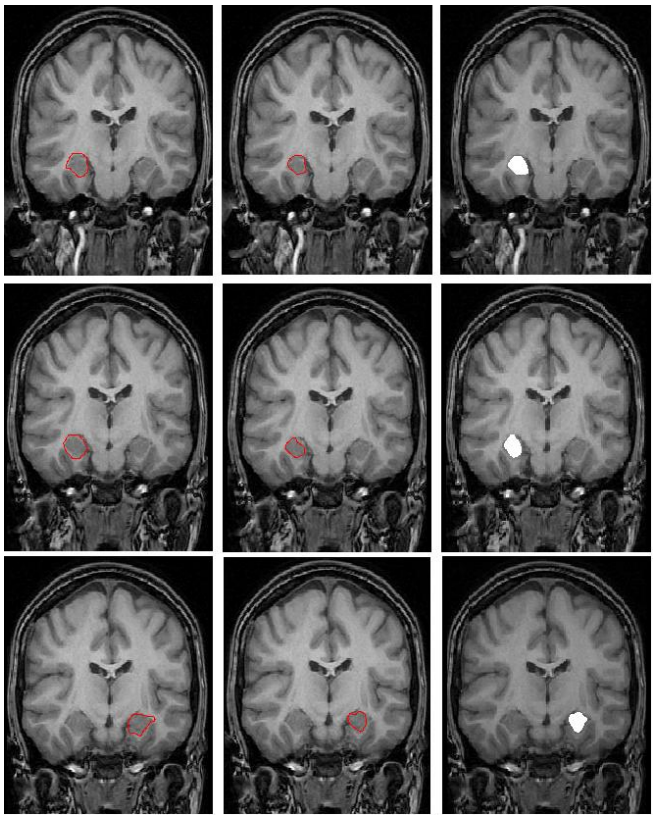

Figure 1. Automatic and expert's hippocampus segmentation results for three different slices on the coronal view. Left: Atlas-based segmentation, Middle: Final level set segmentation, Right: Expert's segmentation. Each row shows a different slice.

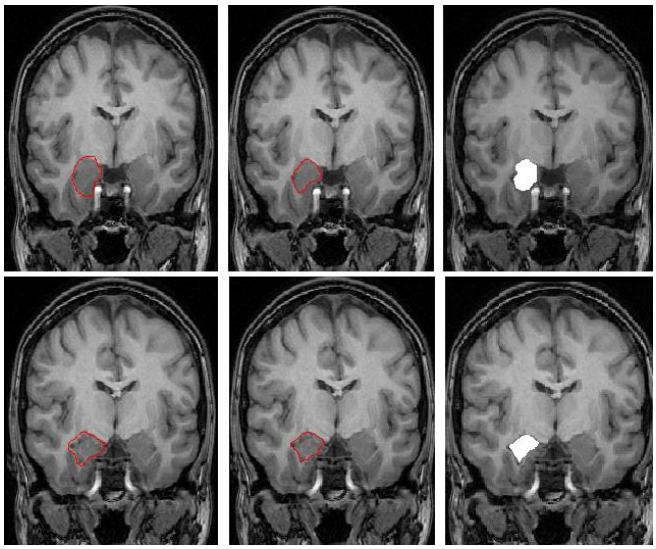

Figure 2. Automatic and expert's amygdala segmentation results for two different slices on the coronal view. Left: Atlas-based segmentation, Middle: Final level set segmentation, Right: Expert's segmentation. Each row shows a different slice.

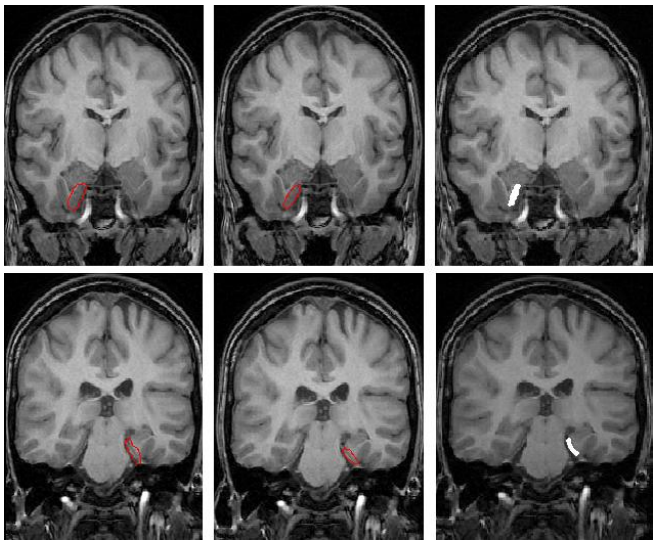

Figure 3. Automatic and expert's Entorhinal cortex segmentation results for two different slices on the coronal view. Left: Atlas-based segmentation, Middle: Final level set segmentation, Right: Expert's segmentation. Each row shows a different slice.

REFERENCES

[1] S. Duchesne, N. Bernasconi, A. Bernasconi and D.L. Collins, "MR-based neurological disease classification methodology: Application to lateralization of seizure focus in temporal lobe epilepsy," *NeuroImage*, vol. 29, pp. 557-566, 2006.

[2] N. Bernasconi, S. Duchesne, A. Janke, "Whole-brain voxel-based statistical analysis of gray matter and white matter in temporal lobe epilepsy," *Neuroimage*, vol. 23, pp. 717–723, 2004.

[3] C. Li, C. Xu, C. Gui, and M. D. Fox, "Level Set Evolution Without Re-initialization: A New Variational Formulation," *IEEE International Conference on Computer Vision and Pattern Recognition*, Vol. 1, pp. 1316-1322, 2005.

[4] J. Ashburner, K. J. Friston, "Voxel-based morphometry-The methods," *NeuroImage*, vol. 11, pp. 805– 821, 2000.

[5] C. D. Good, I. S. Johnsrude, J. Ashburner, N. A. R. Henson, K. J. Friston, R. Frackowiak, "A voxel-based morphometric study of aging in 465 normal adult human brains," *NeuroImage*, vol. 14, pp. 21-36, 2001.

[6] S. Osher, J. A. Sethian, "Fronts propagating with curvaturedependent speed: algorithms based on Hamilton-Jacobi formulations," *J. Comp. Phys.*, vol. 79, pp. 12-49, 1988.

[7] R. Malladi, J. A. Sethian, and B. C. Vemuri, "Shape modeling with front propagation: a level set approach," *IEEE Trans. Patt. Anal. Mach. Intell.*, vol. 17, pp. 158-175, 1995.

[8] R. Malladi, J. A. Sethian, and B. C. Vemuri, "Shape modeling with front propagation: a level set approach," *IEEE Trans. Patt. Anal. Mach. Intell.*, vol. 17, pp. 158-175, 1995.

[9] D. Peng, B. Merriman, S. Osher, H. Zhao, and M. Kang, "A PDE-based fast local level set method," *J. Comp. Phys.*, vol. 155, pp. 410-438, 1999.